

Vision-based Follow-the-Leader

Noah Cowan[†] Omid Shakernia[‡] René Vidal[‡] Shankar Sastry[‡]

[†]Department of Mechanical Engineering
Johns Hopkins University, Baltimore, MD 21218

[‡]Electrical Engineering and Computer Science
University of California, Berkeley, CA 94720

Abstract— We consider the problem of having a group of nonholonomic mobile robots equipped with omnidirectional cameras maintain a desired leader-follower formation. Our approach is to translate the formation control problem from the configuration space into a separate visual servoing task for each follower. We derive the equations of motion of the leader in the image plane of the follower and propose two control schemes for the follower. The first one is based on feedback linearization and is either string stable or leader-to-formation stable, depending on the sensing capabilities of the followers. The second one assumes a kinematic model for the evolution of the leader velocities and combines a Luenberger observer with a linear control law that is locally stable. We present simulation results evaluating our vision-based follow-the-leader control strategies.

I. INTRODUCTION

Birds flock and fish school without explicit communication between individuals. Vision seems to be a critical component in animals' abilities to respond their neighbors' motions so that the entire group maintains a coherent formation. Our long-term goal involves enabling groups of mobile robots to visually maintain formations in the absence of communication, as depicted in Figure 1. Towards that end, we propose and compare two new vision-based controllers that enable one mobile robot to track another, which we dub vision-based follow-the-leader.

Thanks to recent advances in computer vision, one can now address formation control without using explicit communication. For example, Vidal *et al.* [21] consider a formation control scenario in which motion segmentation techniques enable each follower to estimate the image-plane position and velocity of the other robots in the formation, subsequently used for omnidirectional image-based visual servoing (for a tutorial on visual servoing, see [11]). However, the control law in [21] suffers from singular configurations due to nonholonomic constraints on the robots' kinematics.

This paper compares two new visual servo controllers that employ a modification of the image-based coordinate system first presented in [2], which we have modified for omnidirectional imaging.

Our first controller builds directly on the work of Desai *et al.* [5] and Das *et al.* [4], who use input-output feedback linearization on a clever choice of output function – the so-called “separation and bearing” – defined in terms of the absolute Cartesian configurations of the follower and its leader. We show that their approach, which avoids the

above-mentioned singularity [21], can be implemented in image-coordinates, thus simplifying the state estimation problem and enabling the use of image-based visual servoing. Our controller inherits asymptotic convergence from [4] when the forward speed of the leader is known, and, additionally, is leader-to-formation stable (LFS) [20] even without an estimate of the leader velocity.

Our second controller uses a linearization of the leader-follower dynamics, in image-plane coordinates. We note that as long as the leader keeps moving (as also required by [4]), one can stabilize the leader-follower formation with a simple linear control scheme. Of course, the linear controller affords only local convergence guarantees, but our simulations suggest that the controller is quite robust and has a large domain of attraction. Its relative simplicity makes it, in some ways, an appealing alternative to the nonlinear control scheme also presented. Both controllers are exponentially stable and hence we are able to take advantage of results in string and input-to-state stability of formations, which we review in Section I-B.

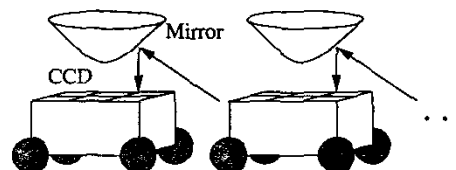


Fig. 1. An omnidirectional vision-based formation of mobile robots.

A. Organization

In Section II we review the imaging model of a central panoramic camera. In Section III we derive the equations of motion of the leader in the image plane of the follower, and modify the coordinate system of [2] for the present context. In Section IV we design a feedback control law using input-output feedback linearization. We show that our control law is either string stable or leader-to-formation stable, depending on the sensing capabilities of the followers. We then linearize the leader-follower dynamics about a nominal *nonzero* forward leader velocity and show that the linearized dynamics are stabilizable and observable. We then design a simple linear controller and observer for the linearized system. In Section V we present simulation results evaluating the performance of our vision-based follow-the-leader control strategies. Section VI concludes the paper.

B. Background

Formation Stability: There is a rich literature addressing the formation control problem when communication among the robots is available, including controller synthesis and stability analysis. For example, Swaroop *et al.* [18] proposed the notion of string stability for line formations and derived sufficient conditions for a formation to be string stable. Pant *et al.* [13] generalized string stability to formations in a planar mesh, through the concept of mesh stability. Tanner *et al.* [19] concentrated on formations in acyclic graphs and studied the effect of feedback and feedforward on the input-to-state stability of the formation. Fax *et al.* [7] analyzed the stability of formations in arbitrary graphs and proposed a Nyquist-like stability criteria that can be derived from the spectral properties of the graph Laplacian. Egerstedt and Hu [6] proposed the use of formation constraint functions to decouple the coordination and tracking problems, while maintaining the stability of the formation.

Decentralized “Local” Control: In addition to [21], [4], Stipanovic *et al.* [16] studied the design of decentralized control laws that result in stable formations, provided that the leader’s desired velocity is known. As well, Fredslund *et al.* [9] evaluate a heuristic method for solving the formation control problem using only local sensing.

II. CENTRAL PANORAMIC IMAGING MODEL

Central panoramic cameras are realizations of omnidirectional vision systems that combine a mirror and a lens and have a unique effective focal point. It was shown in [10] that the image of a 3D point obtained by calibrated central panoramic cameras is given by the mapping

$$\pi_1(q) := \frac{1}{-q_3 + \xi\|q\|} \begin{bmatrix} q_1 \\ q_2 \end{bmatrix} \quad (1)$$

where $\pi_1 : \mathbb{R}^3 \rightarrow \mathbb{R}^2$ and $\xi \in [0, 1]$ is a camera parameter. Notice that $\xi = 0$ corresponds to perspective projection and $\xi = 1$ corresponds to para-catadioptric projection (parabolic mirror with orthographic lens).

It was shown in [15] that by lifting the image point $p \in \mathbb{R}^2$ onto the surface of the virtual retina defined by

$$f_\xi(p) := \frac{-1 + \xi^2\|p\|^2}{1 + \xi\sqrt{1 + (1 - \xi^2)\|p\|^2}}, \quad (2)$$

one can compute the *back-projection ray* $b = [p^T, f_\xi(p)]^T$ such that $\lambda b = q$, where $\lambda = -q_3 + \xi\|q\|$ is the scale lost in the central panoramic projection (see Figure 2). Assume we know the type of camera on the robots, *i.e.* we know ξ , and define the mappings $\pi_2 : \mathbb{R}^2 \rightarrow \mathbb{R}^2$ and $\pi_3 : \mathbb{R}^3 \rightarrow \mathbb{R}^2$ as

$$\pi_2(p) := \frac{1}{f_\xi(p)} p, \quad \pi_3(q) := -\pi_2 \circ \pi_1(q) = \frac{1}{-q_3} \begin{bmatrix} q_1 \\ q_2 \end{bmatrix}, \quad (3)$$

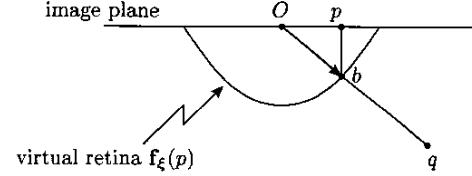


Fig. 2. Central panoramic projection model.

respectively. Notice that π_3 is simply (calibrated) perspective projection, which we obtained by “unwarping” the central panoramic image.

Suppose a central panoramic camera is attached to a mobile robot such that its optical axis is parallel to the z -axis (pointing up). Let the center of the camera be located at $q_3 = 0$ and the ground plane, $\mathcal{G} = \{q \in \mathbb{R}^3 : q_3 = -\zeta\}$, where $\zeta > 0$. By restricting π_3 to $\mathcal{G} \simeq \mathbb{R}^2$, we get the (trivial) diffeomorphism $\pi := \pi_3|_{\mathcal{G}}$, which can be written

$$\pi : \mathbb{R}^2 \rightarrow \mathbb{R}^2, \quad \pi(q) = \frac{1}{\zeta} \begin{bmatrix} q_1 \\ q_2 \end{bmatrix}. \quad (4)$$

In other words, the fairly complicated central panoramic camera model (1) can be easily remapped so that when viewing the ground plane from above, the camera acts as a linear scaling of the coordinates.

III. RELATIVE LEADER-FOLLOWER KINEMATICS

In order to design vision-based follow-the-leader control laws, we need to know the equations governing the motion of the leader in the image plane of the moving follower. In this section, we derive the relative kinematics between the leader and follower in task space and combine them with the camera model described in the Section II.

A. Relative Kinematics in SE(3)

Let $(R_f, T_f) \in SE(3)$ and $(R_\ell, T_\ell) \in SE(3)$ be the pose of the follower and leader, respectively, with respect to a fixed reference frame. Also let $q_\ell \in \mathbb{R}^3$ be the coordinates of a point on the leader written in the *leader frame*, and $q_f \in \mathbb{R}^3$ be the coordinates of the same point in the *follower frame*. Then we have

$$q_f = Rq_\ell + T, \quad (5)$$

where $(R, T) \in SE(3)$ is the pose of the leader relative to the follower in the *follower frame* given by

$$R := R_f^T R_\ell, \quad T := R_f^T (T_\ell - T_f). \quad (6)$$

If we assume that the point q_ℓ is fixed with respect to the leader frame, *i.e.* $\dot{q}_\ell = 0$, then differentiating the relative pose in (5) yields¹

$$\begin{aligned} \dot{q}_f &= \dot{R}q_\ell + \dot{T} \\ &= R(\widehat{\Omega}_\ell q_\ell + V_\ell) - (\widehat{\Omega}_f q_f + V_f), \end{aligned} \quad (7)$$

¹ $\widehat{\Omega} \in so(3)$ is the skew-symmetric matrix generating the cross product, *i.e.* $\widehat{\Omega}q = \Omega \times q$ for all $q \in \mathbb{R}^3$ [12].

where

$$\begin{aligned}\widehat{\Omega}_f &:= R_f^T \dot{R}_f, & V_f &:= R_f^T \dot{T}_f, \\ \widehat{\Omega}_\ell &:= R_\ell^T \dot{R}_\ell, & V_\ell &:= R_\ell^T \dot{T}_\ell,\end{aligned}\quad (8)$$

are the *body* velocities of the follower and leader, i.e. (V_f, Ω_f) , is the velocity of the follower in the follower frame, and (V_ℓ, Ω_ℓ) , is the velocity of the leader in the leader frame. Furthermore, since $\widehat{\Omega}q = -\widehat{q}\Omega$, we have that the coordinates of the fixed point on the leader evolve in the coordinate frame of the follower according to:

$$\dot{q}_f = [-I_{3 \times 3} \quad \widehat{q}_f] \begin{bmatrix} V_f \\ \Omega_f \end{bmatrix} - R [-I_{3 \times 3} \quad \widehat{q}_\ell] \begin{bmatrix} V_\ell \\ \Omega_\ell \end{bmatrix}. \quad (9)$$

Now consider the case that the origin of the follower frame is *not* at its spinning point (i.e. the point about which the follower rotates). Suppose the coordinates of the spinning point are $-q_\delta \in \mathbb{R}^3$ in the follower frame. If $v_f, \omega_f \in \mathbb{R}^3$ are the linear and angular velocities at the spinning point (these are typically control inputs), then it is direct to show that the body velocities at the origin of the follower frame are:

$$\Omega_f = \omega_f, \quad V_f = \widehat{q}_\delta \omega_f + v_f. \quad (10)$$

Therefore, the coordinates of the point on the leader in the follower's frame evolve as:

$$\dot{q}_f = [-I_{3 \times 3} \quad (\widehat{q}_f + \widehat{q}_\delta)] \begin{bmatrix} v_f \\ \omega_f \end{bmatrix} - R [-I_{3 \times 3} \quad \widehat{q}_\ell] \begin{bmatrix} V_\ell \\ \Omega_\ell \end{bmatrix}. \quad (11)$$

This equation will be useful for controlling nonholonomic mobile robots where v_f is restricted to some subspace of \mathbb{R}^3 .

B. Relative Kinematics for Unicycles in SE(2)

Consider the mobile robots are "unicycles" moving in the ground plane. For simplicity, assume the point being tracked on the leader is the origin of the leader frame, i.e. $q_\ell = 0$. The leader's body velocity is given by:

$$\Omega_\ell = [0 \quad 0 \quad \omega_\ell]^T, \quad V_\ell = [v_\ell \quad 0 \quad 0]^T, \quad (12)$$

where $v_\ell, \omega_\ell \in \mathbb{R}$ are the leader's control inputs.

Consider that the origin of the follower frame is not at its spinning point. By choosing the spinning point to be at $q_\delta = (-\delta, 0, 0)^T$ in the follower frame, it follows from (10) that the follower's body velocities are given by:

$$\Omega_f = \begin{bmatrix} 0 \\ 0 \\ 1 \end{bmatrix} \omega_f, \quad V_f = \begin{bmatrix} 1 & 0 \\ 0 & \delta \\ 0 & 0 \end{bmatrix} \begin{bmatrix} v_f \\ \omega_f \end{bmatrix}, \quad (13)$$

where $v_f, \omega_f \in \mathbb{R}$ are the follower's control inputs.

In an abuse of notation, drop the z -axis entry to consider $q_f, q_\ell \in \mathbb{R}^2$. Further, if $\theta := \theta_\ell - \theta_f$ is the orientation of the leader in the coordinate frame of the follower, we have

$$R = \begin{bmatrix} \cos \theta & -\sin \theta \\ \sin \theta & \cos \theta \end{bmatrix} \in \text{SO}(2). \quad (14)$$

Thus, the coordinates of the point on the leader in the coordinate frame of the follower with control actions $(v_f, \omega_f) \in \mathbb{R}^2$ evolve according to:

$$\begin{aligned}\dot{q}_f &= \begin{bmatrix} -1 & -q_{f2} \\ 0 & (q_{f1} + \delta) \end{bmatrix} \begin{bmatrix} v_f \\ \omega_f \end{bmatrix} - R \begin{bmatrix} -1 & -q_{\ell 2} \\ 0 & q_{\ell 1} \end{bmatrix} \begin{bmatrix} v_\ell \\ \omega_\ell \end{bmatrix} \\ \dot{\theta} &= \omega_\ell - \omega_f.\end{aligned}\quad (15)$$

C. Relative Kinematics in the Image Plane

The following image-based coordinate system for relative displacements in SE(2) is a simplification of the more general image-based coordinate system for SE(3) given by Cowan and Chang [2]. For the present case, we assume that the follower can measure the projection of a pair of features the leader. The first point, measured q_f in the follower frame, is at the spinning point of the leader, i.e. the same point is expressed in leader's frame $q_\ell = 0$, as described above. For simplicity, the second feature point is aligned along the leader's x -axis, and the orientation of the pair of features on the image plane is given by ϕ . Hence we have the camera mapping, $c: \text{SE}(2) \rightarrow \text{SE}(2)$, relating Cartesian variables $(q_f, \theta) \in \text{SE}(2)$ to image variables $(p, \phi) \in \text{SE}(2)$ via the diffeomorphism,

$$(p, \phi) = c(q_f, \theta) := (\pi(q_f), \theta) = \left(\frac{1}{\zeta} q_f, \phi \right), \quad (16)$$

where π is given by (4). The Jacobian matrix of c is given trivially by

$$J = \begin{bmatrix} \frac{1}{\zeta} I_{2 \times 2} & 0 \\ 0 & 1 \end{bmatrix}. \quad (17)$$

Recalling that $q_\ell = 0$, the leader-follower kinematics (15) may now be mapped to the image plane as

$$\begin{aligned}\dot{p} &= \frac{1}{\zeta} \begin{bmatrix} -1 & -\zeta p_2 \\ 0 & (\zeta p_1 + \delta) \end{bmatrix} \begin{bmatrix} v_f \\ \omega_f \end{bmatrix} + \frac{1}{\zeta} \begin{bmatrix} \cos \phi \\ \sin \phi \end{bmatrix} v_\ell \\ \dot{\phi} &= \omega_\ell - \omega_f.\end{aligned}\quad (18)$$

In the following section, we design two controllers for system (18). To simplify notation, assume without loss of generality that $\zeta = 1$, and let $x^T = [x_1, x_2, x_3] = [q_{f1}, q_{f2}, \phi] \in \text{SE}(2)$ so that (15) becomes

$$\begin{bmatrix} \dot{x}_1 \\ \dot{x}_2 \\ \dot{x}_3 \end{bmatrix} = \begin{bmatrix} -1 & -x_2 \\ 0 & x_1 + \delta \\ 0 & -1 \end{bmatrix} u + \begin{bmatrix} \cos x_3 & 0 \\ \sin x_3 & 0 \\ 0 & 1 \end{bmatrix} d, \quad (19)$$

where $u = (u_1, u_2)^T = (v_f, \omega_f)^T$ is the follower's linear and angular velocity inputs, and $d = (d_1, d_2)^T = (v_\ell, \omega_\ell)^T$ is the disturbance due to the leader's velocity.

IV. CONTROLLER DESIGN

We present two approaches to controlling (19). The first approach is based on a simple coordinate transformation of the image variables, similar to the task-space "separation and bearing" coordinate system found in [5]. In

the new coordinate system, the problem of keeping the leader within the follower's field-of-view and preventing leader-follower collisions may be naturally encoded. Our potential-function based controller asymptotically tracks a moving leader while maintaining visibility and avoiding mutual collision. For the second approach, we take a local point of view and linearize the system around a nominal leader trajectory, and show that the resulting system is stabilizable and observable. We show that both solutions require a moving leader, and are leader-to-formation stable in the sense defined in [20].

A. Input/Output Feedback Linearization

Image-based separation and bearing: To model those relative configurations for which the leader and follower are not coincident, let $\mathcal{X} = \{x = [x_1, x_2, x_3]^T \in \text{SE}(2) : x_1^2 + x_2^2 > 0\}$. Let $\mathcal{Y} = \mathbb{R}^+ \times \text{S}^1 \times \text{S}^1$ and consider the transformation $h : \mathcal{X} \rightarrow \mathcal{Y}$ given by

$$h(x) := [\sqrt{x_1^2 + x_2^2} \quad x_3 + \arctan2(x_2, x_1) \quad x_3]^T,$$

where $\arctan2$, implemented for example in MATLAB and C, is the natural extension of the arctangent function to all four quadrants. The inverse

$$h^{-1}(y) = \begin{bmatrix} y_1 \cos(y_2 - y_3) \\ y_1 \sin(y_2 - y_3) \\ y_3 \end{bmatrix}$$

may be found by direct computation, and is well defined for all $y = [y_1, y_2, y_3]^T \in \mathcal{Y}$, and thus h is a homeomorphism from \mathcal{X} to \mathcal{Y} .

Finally, note that

$$D_x h(x) = \begin{bmatrix} \frac{x_1}{\sqrt{x_1^2 + x_2^2}} & \frac{x_2}{\sqrt{x_1^2 + x_2^2}} & 0 \\ -\frac{x_2}{x_1^2 + x_2^2} & \frac{x_1}{x_1^2 + x_2^2} & 1 \\ 0 & 0 & 1 \end{bmatrix}$$

and therefore $|Dh| = (x_1^2 + x_2^2)^{-\frac{1}{2}}$, which is nonzero and well defined for $x \in \mathcal{X}$, and thus at each point $x \in \mathcal{X}$, h is a local diffeomorphism. Since h is a local diffeomorphism at every point in the domain and a global homeomorphism, h is a global diffeomorphism. The first two components (y_1, y_2) are called the *separation* and *bearing*, respectively, similar to that defined in [4], [5], [8].

Transformed dynamics: Consider the system (19) written as

$$\dot{x} = f(x)u + g(x)d$$

with $x \in \text{SE}(2)$. Let $y = h(x)$ and note that

$$\dot{y} = D_x h(x)f(x)u + D_x h(x)g(x)d \quad (20)$$

where direct computation yields

$$D_x h(x)f(x) = \begin{bmatrix} F \\ -e_2^T \end{bmatrix} \quad \text{and} \quad D_x h(x)g(x) = \begin{bmatrix} G \\ e_2^T \end{bmatrix}$$

where $e_2 = [0, 1]^T$ and

$$F = \begin{bmatrix} -\frac{x_1}{y_1} & \frac{x_2 \delta}{y_1} \\ \frac{x_2}{y_1} & \frac{x_1 \delta}{y_1} \end{bmatrix}, \quad G = \begin{bmatrix} \frac{x_1 \cos x_3 + x_2 \sin x_3}{y_1} & 0 \\ \frac{x_1 \sin x_3 - x_2 \cos x_3}{y_1} & 1 \end{bmatrix}.$$

Suppose that the leader's velocity, d , is available to the follower for control, either by using optical flow [21], communication or an extended Kalman filter [4]. Note that $\det(F) = -\delta/y_1$ is well defined and non-zero on \mathcal{X} as long as the follower camera is not at the spinning point ($\delta \neq 0$), and thus one may consider the input transformation $u = F^{-1}(\tilde{u} - Gd)$. This yields, by direct substitution

$$\dot{y} = \begin{bmatrix} I_{2 \times 2} \\ -\frac{\sin(y_2 - y_3)}{\delta} & -y_1 \frac{\cos(y_2 - y_3)}{\delta} \end{bmatrix} \tilde{u} + \begin{bmatrix} 0_{2 \times 2} \\ \frac{\sin \phi}{y_1 \delta} & 1 + y_1 \frac{\cos(y_2 - y_3)}{\delta} \end{bmatrix} d. \quad (21)$$

Consider the two-dimensional system output given by the separation and bearing, namely $z = [z_1, z_2]^T \equiv [y_1, y_2]^T \in \text{S}^1 \times \mathbb{R}^+$, which has a well-defined relative degree of one. In local coordinates on $\text{S}^1 \times \mathbb{R}^+$ the "feedback linearized" output dynamics are given by

$$\dot{z} = \tilde{u}. \quad (22)$$

Collision avoidance and visibility: Following [3], we apply the machinery of *navigation functions* (NF) [14] to the vision-based control problem. In this case, we restrict the navigation function to the simple 2D output dynamics in (22). To model all of those image-plane configurations for which the leader and follower maintain a safe separation (to avoid collisions) and remain close enough to maintain good visibility [3], consider the compact manifold with boundary $\mathcal{D} = \{x \in \mathcal{X} : r_{\min}^2 \leq x_1^2 + x_2^2 \leq r_{\max}^2\} \subset \mathcal{X}$, where $0 < r_{\min} < r_{\max}$. Consider the image of \mathcal{D} given by $\mathcal{I} = h(\mathcal{D}) = \{y \in \mathcal{Y} : r_{\min} \leq y_1 \leq r_{\max}\}$. Note that $y \in \mathcal{I}$ if and only if the output stays in the compact set $z \in \mathcal{Z} = [r_{\min}, r_{\max}] \times \text{S}^1$.

Roughly speaking (for a formal definition, see [14]) an NF is a twice differentiable, nondegenerate artificial potential function that has a unique global minimum of 0 on some goal set, and reaches its maximum value of 1 on some obstacle set. Let $\varphi \in C^2[\mathcal{Z}, [0, 1]]$ be a such a function on \mathcal{Z} . For example, let $\sigma(x) = x/(1+x)$ and one easily checks that

$$\varphi(z) = \sigma \left(\frac{k_1(z_1 - z_1^*)^2}{(r_{\max} - z_1)(z_1 - r_{\min})} + k_2(1 - \cos(z_2 - z_2^*)) \right)$$

is an NF ([3], Appendix I), where z^* is the "desired" image-based separation and bearing. Finally, we let

$$\tilde{u} = -\nabla \varphi \quad (23)$$

which guarantees that z will converge to the minima of φ (for all initial conditions except a set of measure zero).

Of course since φ is nondegenerate, the z dynamics are exponentially stable at the goal point.

String stability: By a small perturbation analysis, one can show that the internal dynamics of y_3 from (21) are stable as well [8]. In this case, consider a *string* of vision-based robots, each following the robot ahead of it. Since the robots are kinematic unicycles, and each pair in the string is exponentially stable, one can see that the interconnected system is exponentially string stable [18]. Of course, as a consequence of the topology of \mathcal{X} , global exponential convergence for a smooth feedback law on this system is impossible.

Input-to-formation stability: However, the above mentioned approaches to estimating the feedforward term due to the leader speed are sensitive to noisy vision-based measurements. Thus, we will design a controller assuming zero leader velocity, and then show that the resulting system is Leader-to-Formation stable [20].

Consider the following controller *without* the feedforward disturbance cancellation term, i.e. $u = F^{-1}\tilde{u}$. Letting $\tilde{u} = -\nabla\varphi$ as before, we have the following closed loop dynamics:

$$\dot{z} = -\nabla\varphi + Gd \quad (24)$$

Observe (20) and note that the disturbance term is bounded, i.e. $\|Gd\| \leq \|(v_\ell, \omega_\ell)^T\|$, and the disturbance-free system is locally exponentially stable. Thus, it follows that the controller renders the system Leader-to-Formation stable [20].

B. Observer-based Linear Controller

Let us augment the state of the system x with the leader velocities $(x_4, x_5) = (v_\ell, \omega_\ell)$. Assuming, for simplicity, that the follower's camera is on its spinning point, i.e. $\delta = 0$, then (19) becomes

$$\begin{bmatrix} \dot{x}_1 \\ \dot{x}_2 \\ \dot{x}_3 \end{bmatrix} = \begin{bmatrix} -1 & -x_2 \\ 0 & x_1 \\ 0 & -1 \end{bmatrix} u + \begin{bmatrix} \cos x_3 & 0 \\ \sin x_3 & 0 \\ 0 & 1 \end{bmatrix} \begin{bmatrix} x_4 \\ x_5 \end{bmatrix}. \quad (25)$$

We treat the leader's translational and angular velocities (x_4, x_5) as states with linear dynamics perturbed by *unknown and arbitrary*, but bounded, disturbances. In other words we model the leader velocities as

$$\begin{bmatrix} \dot{x}_4 \\ \dot{x}_5 \end{bmatrix} = \begin{bmatrix} -(x_4 - s) \\ -x_5 \end{bmatrix} + \begin{bmatrix} a_1 \\ a_2 \end{bmatrix} \quad (26)$$

where s is the "nominal" forward speed of the leader, and $[a_1, a_2]^T \in \mathbb{R}^2$ represents an unknown leader acceleration. Let $y = \tilde{h}(x) = [x_1, x_2]^T$ be the system output, and combine (25) and (26), to yield

$$\dot{x} = \tilde{f}(x, u) + a \quad (27)$$

$$y = \tilde{h}(x) \quad (28)$$

where $a = [0, 0, 0, a_1, a_2]^T$ is considered as an unknown but bounded disturbance.

Consider the desired formation described by the equilibrium to (27) given by $x^* = [x_1^*, x_2^*, 0, s, 0]^T$ and $u^* = [s, 0]^T$, where (x_1^*, x_2^*) is the desired location of the leader in the follower frame. The linearized dynamics are given by

$$\begin{aligned} \dot{\tilde{x}} &= A\tilde{x} + B\tilde{u} \\ \tilde{y} &= C\tilde{x}, \end{aligned} \quad (29)$$

where $\tilde{x} = (x - x^*)$ and $\tilde{u} = (u - u^*)$, with system matrices $A = D_x f(x^*, u^*)$, $B = D_u f(x^*, u^*)$ and $C = D_x \tilde{h}(x^*)$ are of the form

$$\begin{aligned} A &= \begin{bmatrix} A_c & A_{12} \\ 0_{3 \times 3} & A_{\bar{c}} \end{bmatrix}, \quad B = \begin{bmatrix} B_c \\ 0_{2 \times 2} \end{bmatrix} \\ C &= [I_{2 \times 2} \quad 0_{2 \times 3}]. \end{aligned} \quad (30)$$

According to Brockett, nonholonomic systems, such as the model in this paper, are not stabilizable to a stationary point via continuous feedback [1]. However, a stabilizing feedback may exist for tracking a given trajectory [17]. For example, if $s \neq 0$, (A, C) is completely observable, and (A, B) is stabilizable. In other words the leader has to be moving for the follower to achieve asymptotic tracking.

The system (29-30) is in Kalman controllable form and the uncontrollable states associated with $A_{\bar{c}}$ correspond to the leader dynamics. Thus, given (A, B, C) , one may design a controller and observer pair using any of the well-known linear control systems design techniques. In Section V, we evaluate via simulation a controller design that uses a full-state Luenberger observer.

Estimating Leader Velocity: To get the leader speed, there are several alternatives. One possibility would be to use optical flow to estimate the leaders velocity, as done in [21]. However, such approaches will be sensitive to noisy measurements. Alternatively, one could use communication between the leader and followers, requiring communication equipment.

Rather than taking the centralized or optical flow approaches, our formulation allows us to design an observer and controller based only the follower's measurement of the leader, namely $y = (x_1, x_2)^T$. From those two numbers, an observer can be used to estimate the relative leader-follower angle x_3 , and leader's linear and angular velocities (x_4, x_5) . The estimator combined with state feedback form a linear regulator.

Leader-to-Formation Stability (LFS): Assume we have designed a stabilizing state feedback for (30), that feeds back the output of a stable observer. In order to tackle the LFS problem, we place a mild assumption on the leader dynamics, namely that the leader *acceleration*, a , be bounded. This means that the leader must follow continuous velocity trajectories. Given this restriction, local LFS becomes a trivial problem – it is inherited directly from the bounded-input-bounded-output (BIBO) stability of the stable linear system.

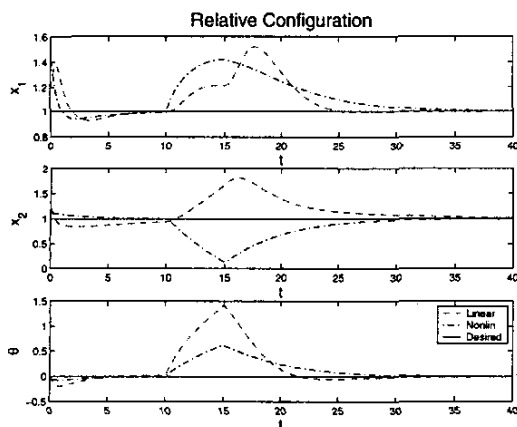


Fig. 3. Performance comparison for the linear observer-controller pair versus the nonlinear controller.

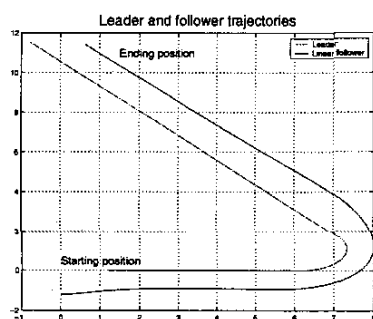


Fig. 4. Leader and follower trajectories for the linear controller-observer.

V. EXPERIMENTS

We briefly compare the two controllers described in Sections IV. In both cases, the performance was similar, and via many simulations, we have not been able to cause the linear algorithm to fail. This leads us to believe that the linear algorithm has a substantial domain of attraction, and its relative simplicity makes it appealing.

Figure 3 shows the error trajectory for both the linear and nonlinear controllers described in the previous section. In both cases, the leader is moving at a constant forward speed that is known to both followers. For the first 10 seconds, the leader is not rotating, but at $t = 10$ the leader executes a simple maneuver, rotating at a constant angular velocity for 5 seconds (while continuing to move forward). At $t = 15$ the leader continues with no angular velocity.

For both the linear and nonlinear controllers, the angular velocity maneuver is unknown and unanticipated by the follower. Nevertheless, both the linear and nonlinear controllers “keep up” with the leader and when the leader completes its maneuver, both followers asymptotically converge to the desired formation, as shown in Figure 4.

VI. CONCLUSION

We have presented a novel approach to vision-based formation control of nonholonomic robots equipped with central panoramic cameras. Our approach assumes a desired

formation in the image plane and uses omnidirectional visual servoing for tracking. We proposed two control strategies and showed that they are either string, leader-to-formation, or locally stable depending on the sensing capabilities of the followers. We presented simulations evaluating our vision-based follow-the-leader controllers.

ACKNOWLEDGMENTS

The first author was supported in part by DARPA/ONR under grants N00014-98-1-0747 and N66001-00-C8026, and NSF under grant ECS-9873474. The remaining authors thank the support of ONR grant N00014-00-1-0621.

VII. REFERENCES

- [1] R. Brockett. Asymptotic stability and feedback stabilization. In R. Brockett, R. Millman, and H. Sussman, editors, *Differential Geometric Control Theory*. Springer-Verlag, 1983.
- [2] N. Cowan and D. Chang. *Second Workshop on Control Problems in Robotics and Automation*, chapter Toward Geometric Visual Servoing. Springer-Verlag, 2002.
- [3] N. Cowan, J. Weingarten, and D. Koditschek. Visual servoing via navigation functions. *IEEE Transactions on Robotics and Automation*, 18(4):521–533, 2002.
- [4] A. Das, R. Fierro, V. Kumar, J. Ostrowski, J. Spletzer, and C. J. Taylor. A vision-based formation control framework. *IEEE Transactions on Robotics and Automation*, 18(5):813–825, 2002.
- [5] J. Desai, J. Ostrowski, and V. Kumar. Modeling and control of formations of nonholonomic robots. *IEEE Transactions on Robotics and Automation*, 17(6):905–908, 2001.
- [6] M. Egerstedt and X. Hu. Formation constrained multiagent control. *IEEE Trans. on Robotics and Automation*, 17(6):947–951, 2001.
- [7] A. Fax and R. Murray. Graph Laplacians and stabilization of vehicle formations. In *IFAC World Congress*, 2002.
- [8] R. Fierro, P. Song, A. Das, and V. Kumar. Cooperative control of robot formations. In *Cooperative Control and Optimization*, volume 66, chapter 5, pages 73–93. Kluwer Academic Press, 2002.
- [9] J. Fredslund and M. J. Mataric. A general algorithm for robot formations using local sensing and minimal communication. *IEEE Transactions on Robotics and Automation*, 18(5):837–846, 2002.
- [10] C. Geyer and K. Daniilidis. A unifying theory for central panoramic systems and practical implications. In *Proceedings of the European Conference on Computer Vision*, Dublin, Ireland, 2000.
- [11] S. Hutchinson, G. Hager, and P. Corke. A tutorial on visual servo control. *IEEE Trans. on Robotics and Aut.*, 12(5):651–670, 1996.
- [12] R. Murray, Z. Li, and S. Sastry. *A Mathematical Introduction to Robotic Manipulation*. CRC Press, 1993.
- [13] A. Pant, P. Seiler, T. Koo, and K. Hedrick. Mesh stability of UAV clusters. In *American Control Conference*, pages 62–68, 2001.
- [14] E. Rimon and D. Koditschek. Exact robot navigation using artificial potential fields. *Trans. on Robotics and Aut.*, 8(5):501–518, 1992.
- [15] O. Shakernia, R. Vidal, and S. Sastry. Multibody motion estimation and segmentation from multiple central panoramic views. In *IEEE International Conference on Robotics and Automation*, 2003.
- [16] D. Stipanovic, G. Inalhan, R. Teo, and C. Tomlin. Decentralized overlapping control of a formation of unmanned aerial vehicles. In *IEEE Conf. on Decision and Control*, pages 2829–2835, 2002.
- [17] H. J. Sussmann and W. Liu. Limits of highly oscillatory controls and the approximation of general paths by admissible trajectories. In *IEEE Conf. on Decision and Control*, pages 437–442, 1991.
- [18] D. Swaroop and J. Hedrick. String stability of interconnected systems. *IEEE Trans. on Automatic Control*, 41:349–357, 1996.
- [19] H. Tanner, V. Kumar, and G. Pappas. The effect of feedback and feedforward on formation ISS. In *IEEE ICRA*, pp. 3448–3453, 2002.
- [20] H. Tanner, G. Pappas, and V. Kumar. Leader-to-formation stability. *IEEE Transactions on Robotics and Automation*, 2003. Submitted.
- [21] R. Vidal, O. Shakernia, and S. Sastry. Formation control of nonholonomic mobile robots with omnidirectional visual servoing and motion segmentation. In *IEEE ICRA*, 2003.